

# Reports

## Particle Track Identification: Application of a New Technique to Apollo Helmets

**Abstract.** *The Apollo helmets are being used to record the dose of heavy particles to which astronauts are exposed on space missions. An improved method for examining and identifying the etched tracks of heavy charged particles consists of replicating tracks and measuring the etching rate as a function of position along the track. Tracks have been observed in Apollo helmets that correspond to ionized atoms heavier than iron.*

Recent reports by Apollo astronauts of lines of light apparently seen with the eyes closed (1) have rekindled interest in possible biological effects of heavily ionizing particles that penetrate the shielding of the spacecraft or space suit during missions outside the earth's magnetosphere. In a dosimetry experiment in progress (2) the plastic Apollo helmets are used as recorders of heavy cosmic-ray particles directly incident on the faces and heads of the astronauts. In this experiment the particle tracks are revealed by chemically etching (3) the interior of the Lexan polycarbonate helmet to produce cone-shaped holes, which are later counted.

We have replicated these tracks, using a silicone rubber that faithfully reproduces the shapes and dimensions of the etched tracks and at the same time allows the tracks to be viewed while placed on a flat surface for ease of observation (4). Alternatively, we can cut out a single track and rotate it on a goniometer so that it can be viewed in profile, as illustrated in Fig. 1.

The procedure for particle identification is based on the fact that the etching rate along a track is a monotonically increasing function of the

primary ionization of the particles (5), so that, if we can measure the ionization point by point along a track, we have information that is more than sufficient to identify the particle. This new method is a simplification of our previous procedure of measuring track lengths to provide measures of the

average ionization along the portions of a track (6).

The ratio of  $V_G$  (the general dissolution rate of the etchant on undamaged plastic) to  $V_T$  (the local rate of attack along the particle track) is the sine of the cone angle  $\theta$  at the corresponding point along the track (3), as illustrated in Fig. 2. The diameter  $D$  at a range  $x$  from the point where the particle comes to rest gives the cone angle at a range  $R$ . By straightforward geometry we can determine  $V_T$ :

$$V_T(R) = V_G[(\tan \theta)^{-2} + 1]^{\frac{1}{2}}$$

Moreover,

$$R = x + \frac{1}{2}D(x)\tan \theta$$

an equation that is needed since  $\theta$  is measured as a function of  $x$  rather than  $R$ . Since

$$\tan \theta = \frac{1}{2}dD/dx$$

a measure of either  $D$  and  $\theta$  or  $D$  and  $dD/dx$  allows  $V_T$  to be found point by point along a track.

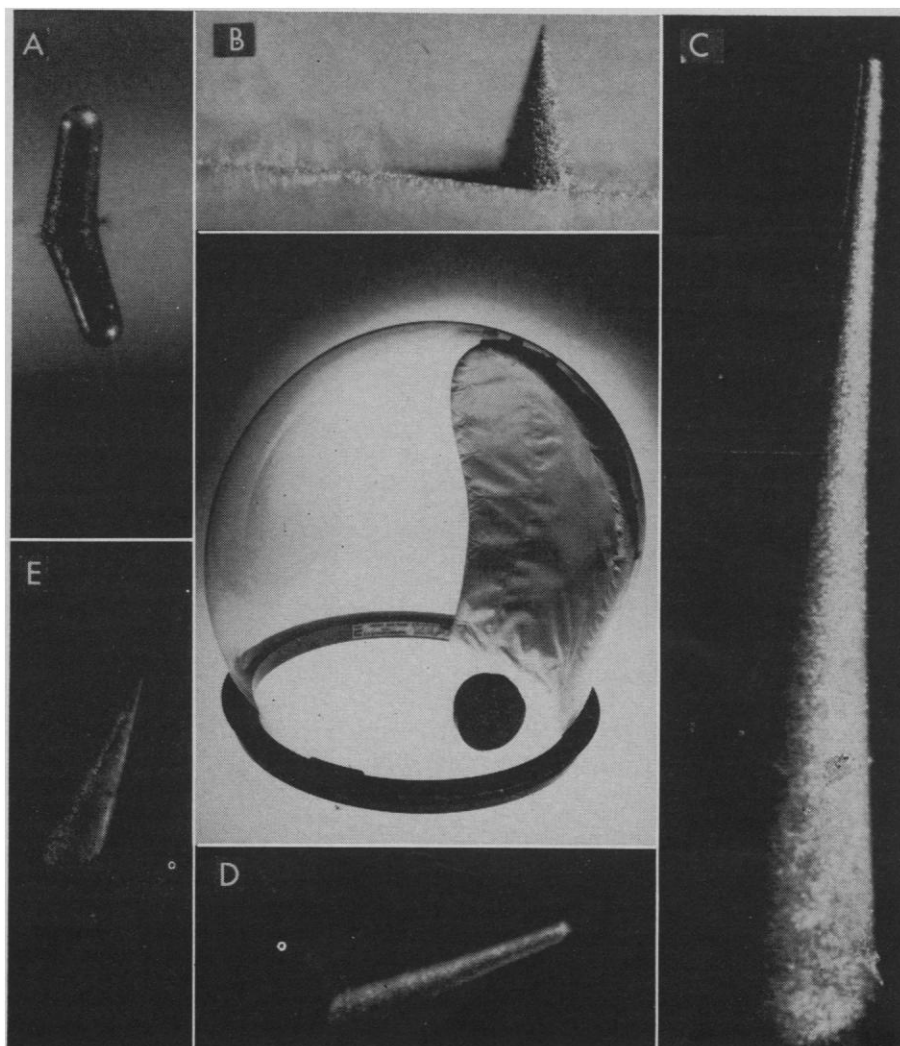


Fig. 1. Cosmic-ray tracks in Apollo helmets. The Apollo 8 helmet of astronaut Lovell, one of several used in a personnel dosimetry experiment, is surrounded by replicas of etched cosmic-ray tracks. Tracks A, D, and E are from the helmets of Apollo 12 astronauts Conrad and Gordon, the other tracks from a control helmet exposed to primary cosmic rays. Track C is from a zinc ion. The lengths (in micrometers) of the track replicas are: A, 350; B, 300; C, 700; D, 600; and E, 480.

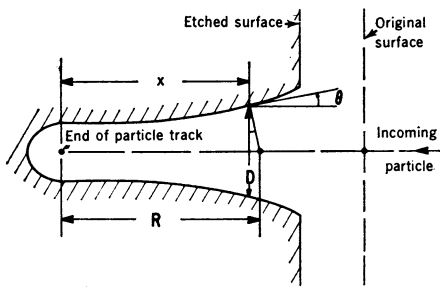


Fig. 2. Diagram illustrating how a measure of a diameter as a function of distance determines the cone angle at positions along an etched track.

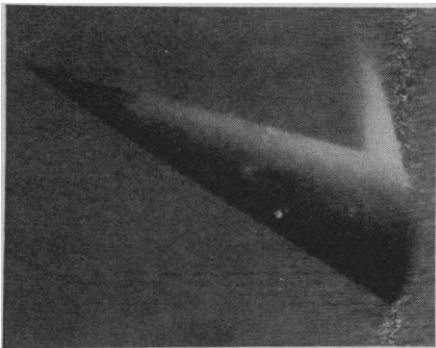


Fig. 3. Replica of an etched cosmic-ray track caused by a nickel ion passing into an Apollo helmet. The track is  $500 \mu\text{m}$  long.

In order to use this procedure to identify particles we would normally compare the observed variations of  $V_T$  with residual range with those observed for known ions, after appropriate allowances for charge and mass differences have been made. For the purposes of this work we have integrated the observed  $V_T$  values so that we might compare these values with track length measurements made previously (5, 7, 8) on cosmic-ray tracks etched with the same solution (1 part 6.25N NaOH to 1 part of ethanol, by volume).

Such intercomparison allows us to infer that the track shown in Fig. 1C is from a zinc ion and the track in Fig. 3 is from a nickel ion. The calibration curves of reference (5) indicate that the charge assignment depends on the angle between the track and the plane of the surface. The silicone rubber replica preserves this angle and allows the proper calibration curve to be selected. The precision or resolution of the charge assignment is good to the nearest atomic number. The true value of the charge is more difficult to assign since the calibration (5) was made on Lexan for which there is a markedly different

processing history (8a) and a different etching time, and for which the number of cosmic-ray particles yields a calibration having a statistical uncertainty in the charge assignment of at least one atomic number, with an uncertainty of two atomic numbers being conceivable but highly unlikely. For tracks with rounded tips the place where the particle came to rest is known, and hence the energy can be determined at each point along the track. This knowledge makes identification more precise than in a case such as that shown in Fig. 3, where the range is uncertain and only the variation in cone angle along the track can be used to decide the range.

There is probably a direct relation between the number of particle tracks and the deactivation of living cells. Experiments (9) have indicated that nuclei are the most vulnerable portions of cells. The likely (but unproved) explanation for this observation is the interference with the replicating properties of long-chain molecules caused by the intense electronic ionization and excitation produced by energetic, massive charged particles.

It has been noted (10) that the same processes determine track formation

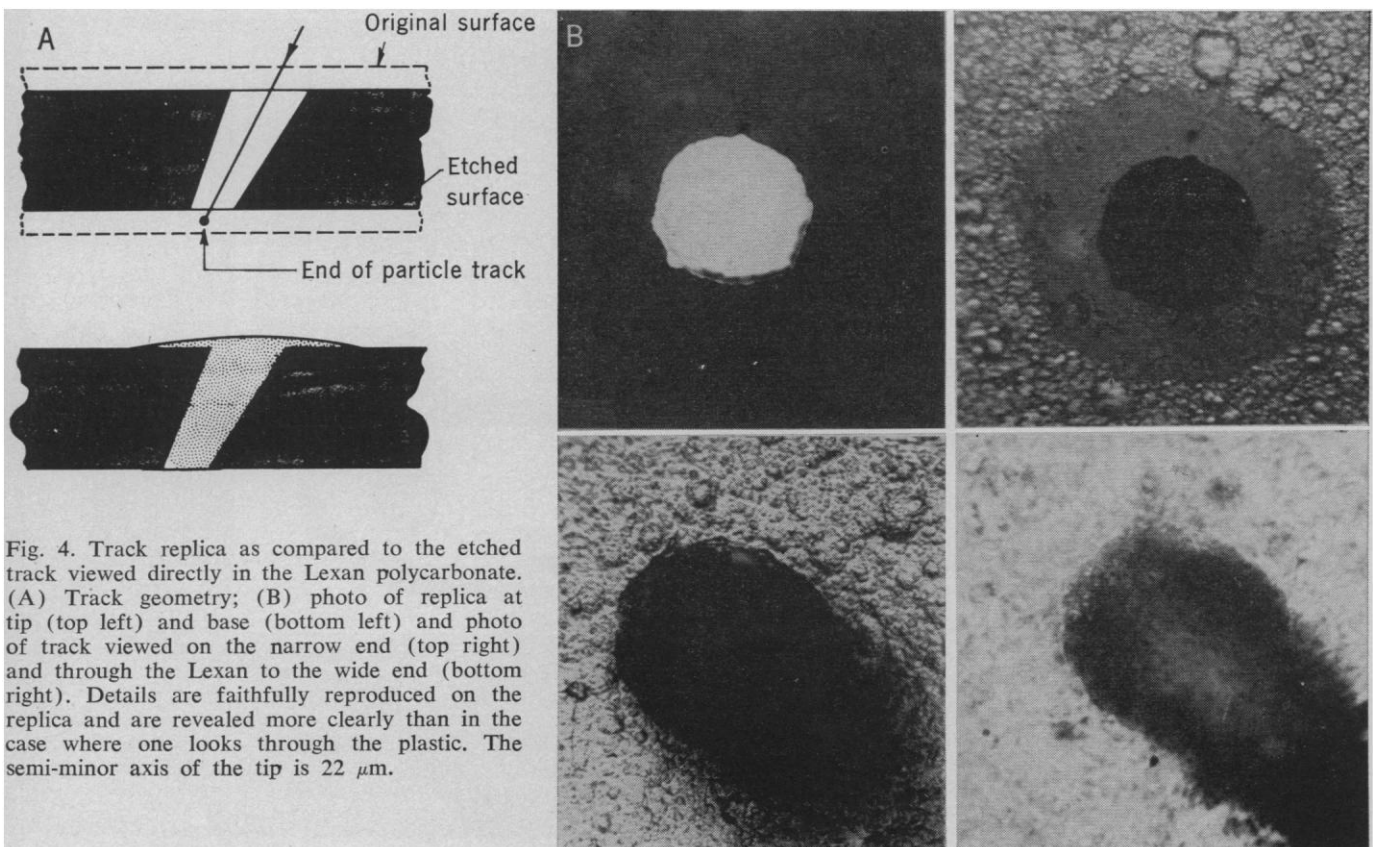


Fig. 4. Track replica as compared to the etched track viewed directly in the Lexan polycarbonate. (A) Track geometry; (B) photo of replica at tip (top left) and base (bottom left) and photo of track viewed on the narrow end (top right) and through the Lexan to the wide end (bottom right). Details are faithfully reproduced on the replica and are revealed more clearly than in the case where one looks through the plastic. The semi-minor axis of the tip is  $22 \mu\text{m}$ .

(11) in polymeric material, since polymers consist of long-chain organic molecules. Therefore, the presence or absence of tracks in plastic adjacent to biological matter (for example, the Apollo helmets) should correlate directly with the presence or absence of damage caused by heavy particles in living cells (10).

Comparison of the curvatures of the track sides reveals that the particle whose track is illustrated in Fig. 3 came from outside the helmet (since looking along the track reveals that the cone angle decreases toward the base) whereas, by contrast, the ion corresponding to the track in Fig. 1C came from within the helmet (cone angle increasing toward the base). Thus, three of the tracks shown in Fig. 1, C, D, and A, represent particles that penetrated through the helmet and came to rest in the opposite side on their way out.

In order for the replica technique to be useful it must faithfully reproduce the shape and dimensions of the etched track. On the basis of an inter-comparison of etched tracks with their replicas, it is clear that the replica does reproduce the dimensions down to submicrometer sizes but that (perhaps due to surface charges) the shapes of slender tracks  $< 2 \mu\text{m}$  in diameter are often bent. Figure 4B shows a tapering track due to a particle that nearly crossed a sheet of Lexan polycarbonate, as sketched in Fig. 4A. A replica was made (as diagrammed in Fig. 4A), gold-coated by evaporation, and photographed. In Fig. 4B the photographs of the replica are compared with those taken directly of the Lexan. Fine detail is reproduced on a micrometer scale. In cellulose nitrate we have successfully replicated conical tracks with lengths up to  $18 \mu\text{m}$  and bases 0.4 to  $0.5 \mu\text{m}$  in diameter.

The replicating procedure makes possible the use of opaque or optically anisotropic plastic sheets as identifiers of particle tracks. Meaningful direct optical measurements of track dimensions are difficult in such materials, for example, Cronar, Melinex, and Mylar; the use of a replica allows accurate measurements to be made (12).

R. L. FLEISCHER  
H. R. HART, JR.  
W. R. GIARD

General Electric Research and  
Development Center,  
Schenectady, New York 12301

#### References and Notes

1. *Science News* (30 May 1970), p. 523.
2. G. M. Comstock, R. L. Fleischer, W. R. Giard, H. R. Hart, Jr., G. E. Nichols, P. B. Price, in preparation.
3. R. L. Fleischer and P. B. Price, *Science* **140**, 1221 (1963).
4. General Electric RTV-11 silicone rubber, Silicone Products Department, Waterford, N.Y. The rubber is applied to the tracks and the system is briefly evacuated to remove dissolved gases and to ensure full penetration.
5. P. B. Price, D. D. Peterson, R. L. Fleischer, C. O'Ceallaigh, D. O'Sullivan, A. Thompson, *Acta Phys. Hungarica Suppl. I* **29**, 417 (1970) (available as General Electric preprint 69-C-299).
6. P. B. Price, R. L. Fleischer, D. D. Peterson, C. O'Ceallaigh, D. O'Sullivan, A. Thompson, *Phys. Rev.* **164**, 1618 (1967); *Phys. Rev. Lett.* **21**, 630 (1968).
7. D. D. Peterson, thesis, Rensselaer Polytechnic Institute (1969).
8. ———, P. B. Price, R. L. Fleischer, unpublished data.
- 8a. Although in principle different varieties of Lexan may have different sensitivities, we find that this is not the case here. Samples of helmet Lexan (9040-112) and of the previously calibrated (5) Lexan (8070-112) gave identical etching response to  $\text{Ne}^{20}$  and  $\text{S}^{32}$  ions from the Yale Heavy Ion Accelerator. The two irradiations were performed at a pressure of 160 mm of oxygen to simulate conditions at the inside of the space helmets during the Apollo missions.
9. P. Todd, *Radiat. Res. Suppl.* **7**, 196 (1967); L. D. Skarsgard, B. A. Kihlman, L. Parker, C. M. Pujara, S. Richardson, *ibid.*, p. 208.
10. R. L. Fleischer, paper presented at the Conference on Space Radiation Biology, Berkeley, Calif., 9-10 Sept. 1965.
11. ———, P. B. Price, R. M. Walker, *J. Appl. Phys.* **36**, 3645 (1965).
12. Even in Lexan, which is an optically more uniform material than the plastics named above, discrepancies exist between measurements on individual tracks when viewed through the material with the track pointing down as compared with the case when the track is pointing up, and one views through the whole sheet thickness (7). Our measurements suggest that the down-pointing position gives numbers that are closer to the true values.
13. We acknowledge helpful conversations with C. P. Bean, J. A. Bergeron, and V. P. Bond. Work supported in part by NASA contract NAS-9-9828.

10 August 1970

## Cubic FeS, a Metastable Iron Sulfide

Abstract. *Studies of the corrosion products of metallic iron formed in the absence of air oxidation in solutions of hydrogen sulfide have revealed the existence of a new phase, cubic FeS, associated with tetragonal iron sulfide,  $\text{Fe}_{1+x}\text{S}$ . This new phase is metastable and has a sphalerite-like structure.*

The initial corrosion product of metallic iron in aqueous solutions of  $\text{H}_2\text{S}$  is tetragonal  $\text{Fe}_{1+x}\text{S}$  (mackinawite). Hexagonal FeS (troilite) appears after a few days at room temperature, or after a few hours at elevated temperature. Finally, cubic  $\text{FeS}_2$  (pyrite) is formed, if an oxidizing agent is present (1, 2).

In experiments of the same type, I observed the formation of a metastable phase, cubic FeS (3). This iron sulfide forms on reagent-grade metallic iron, in 2 or 3 days at room temperature, if the initial concentration of  $\text{H}_2\text{S}$  is greater than  $0.01M$  and the pH is between 4.0 and 4.5. The presence of air or foreign ions (chloride, sulfate) must be avoided.

The x-ray diffraction powder pattern (Table 1) must be taken rapidly, since cubic FeS is metastable when it is not in contact with the solution: the intensity of the reflections decreases by about 10 percent per hour. The  $d$  values and relative intensities are very similar to those of cubic ZnS (sphalerite). The cubic cell parameter, extrapolated against the Nelson and Riley function, is  $a_0 = 5.423 \pm 0.001 \text{ \AA}$  at  $25^\circ\text{C}$ . A very similar value,  $a_0 = 5.4246 \pm 0.0006 \text{ \AA}$ , is deduced from the variation of the cell parameter of the solid solution (Zn,Fe)S (4). The good agreement be-

tween observed and calculated intensities confirms the sphalerite-like structure of cubic FeS.

A comparison of the crystal structures of tetragonal and cubic FeS shows that the formation of the metastable cubic form is favored by epitaxial growth at the interface between the tetragonal iron sulfide and the hydrogen sulfide solution.

Tetragonal  $\text{Fe}_{1+x}\text{S}$  has an anti-PbO

Table 1. X-ray diffraction powder data for cubic FeS (Ni-filtered  $\text{CuK}\alpha$  radiation).  $d$ , Interplanar spacing;  $I/I_0$ , intensity of a given set of planes relative to the strongest intensity.

$hkl$	$d_{\text{obs}}$ ( $\text{\AA}$ )	$d_{\text{calc}}$ ( $\text{\AA}$ )*	$(I/I_0)_{\text{obs}}$	$(I/I_0)_{\text{calc}}^\dagger$
111	3.127	3.131	100	100
200	2.705	2.712	6	5.5
220	1.914	1.917	54	56.9
311	1.634	1.635	36	32.8
222	1.563	1.565	$< 5^\ddagger$	1.1
400	1.354	1.356	8	7.2
331	1.243	1.244	$< 14^\ddagger$	10.5
420	1.212	1.213	$< 2$	0.8
422	1.106	1.107	10	12.8
511-				
333	1.044	1.044	3	7.3
440	0.9581	0.9587	3	4.4
531	0.9161	0.9167	9	8.6
620	0.8570	0.8575	7	8.7

\* Calculated with the extrapolated value of  $a_0 = 5.423 \text{ \AA}$ .  $^\dagger$  Calculated with  $B$  (isotropic temperature factor) =  $1.0 \text{ \AA}^2$ .  $^\ddagger$  Two reflections of  $\text{Fe}_{1+x}\text{S}$  interfere: 211 with 222 (cubic) and 203 with 331 (cubic).